

This discussion paper is/has been under review for the journal Hydrology and Earth System Sciences (HESS). Please refer to the corresponding final paper in HESS if available.

# Elusive drought: uncertainty in observed trends and short- and long-term CMIP5 projections

**B. Orlowsky and S. I. Seneviratne**

Institute for Atmospheric and Climate Science, ETH Zurich, Universitaetsstr. 16,  
8092 Zurich, Switzerland

Received: 23 November 2012 – Accepted: 5 December 2012 – Published: 18 December 2012

Correspondence to: B. Orlowsky (boris.orlowsky@env.ethz.ch)

Published by Copernicus Publications on behalf of the European Geosciences Union.

## Elusive drought

B. Orlowsky and  
S. I. Seneviratne

Title Page

Abstract

Introduction

Conclusions

References

Tables

Figures

◀

▶

◀

▶

Back

Close

Full Screen / Esc

Printer-friendly Version

Interactive Discussion



## Abstract

Recent years have seen a number of severe droughts in different regions around the world, causing agricultural and economic losses, famines and migration. Despite their devastating consequences, the Standardised Precipitation Index (SPI) of these events lies within the range of internal climate variability, which we estimate from simulations from the 5th phase of the Coupled Model Intercomparison Project (CMIP5). In terms of drought magnitude, regional trends of SPI over the last decades remain mostly inconclusive in observations and CMIP5 simulations, although Soil Moisture Anomalies (SMAs) in CMIP5 simulations hint at increased drought in a few regions (e.g. the Mediterranean, Central America/Mexico, the Amazon, North-East Brazil and South Africa). Also for the future, projections of meteorological (SPI) and agricultural (SMA) drought in CMIP5 display large uncertainties over all time frames, generally impeding trend detection. Analogue analyses of the frequencies rather than magnitudes of future drought display, however, more robust signal-to-noise ratios with detectable trends towards more frequent drought until the end of the 21st century in the Mediterranean, South Africa and Central America/Mexico. Other present-day hot spots are projected to become less drought-prone, or to display insignificant changes in drought occurrence. A separation of different sources of uncertainty in drought projections reveals that for the near term, internal climate variability is the dominant source, while the formulation of Global Climate Models (GCMs) generally becomes the dominant source of uncertainty by the end of the 21st century, especially for agricultural (soil moisture) drought. In comparison, the uncertainty in Green-House Gas (GHG) concentrations scenarios is negligible for most regions. These findings stand in contrast to respective analyses for a heat wave indicator, for which GHG concentrations scenarios constitute the main source of uncertainty. Our results highlight the inherent difficulty of drought quantification and the uncertainty of drought projections. However, high uncertainty should not be equated with low drought risk, since potential scenarios include large drought increases in key agricultural and ecosystem regions.

## Elusive drought

B. Orlowsky and  
S. I. Seneviratne

Title Page

Abstract

Introduction

Conclusions

References

Tables

Figures

◀

▶

◀

▶

Back

Close

Full Screen / Esc

Printer-friendly Version

Interactive Discussion



# 1 Introduction

The last decade has witnessed a number of severe drought events, e.g. the 2005 and 2010 droughts of the Amazon (both characterised as “100-yr events”, Marengo et al., 2008; Lewis et al., 2011), the 2009–2011 drought years in China (Barriopedro et al., 2012; Sun and Yang, 2012), the North American “Texas” drought (since 2010, see Peterson et al., 2012; Seneviratne, 2012; Hoerling et al., 2012), the Horn of Africa and Sahel droughts in 2011 (Lyon and DeWitt, 2012), and the recent decade-long drought in Australia (McGrath et al., 2012). In the recent Special Report by the Intergovernmental Panel on Climate Change (IPCC) on *Managing the Risks of Extreme Events and Disasters to Advance Climate Change Adaptation* (SREX), droughts are highlighted as one of the great challenges faced under climate change (IPCC, 2012; Seneviratne et al., 2012), in particular for several hot spot regions that are consistently projected to be more strongly affected by drought in future CMIP5 simulations (e.g. the Mediterranean, Central America/Mexico, the Amazon, North-East Brazil and South Africa). Several of the regions that have either experienced recent drought or are projected to be more strongly affected by drought in the future are important agricultural areas (e.g. central Europe, parts of the US or India; see Monfreda et al., 2008), on which global food production may critically depend in the future (Foley et al., 2011). In addition, drought in the Amazon region has been highlighted as a possible tipping element of the climate system (Lenton et al., 2008), involving potential large feedbacks to the global carbon cycle (Friedlingstein et al., 2006; Poulter et al., 2010). Assessing the uncertainty and likely range of drought projections is therefore of key importance.

In this study we address past and projected future changes in droughts from a variety of perspectives. After introducing the employed data and indicators, we first identify drought hot spots by compiling information on general drought exposition, land use and future drought projections (Sect. 2). For these hot spots, after a global robustness assessment of drought trends, we investigate the recent past w.r.t. drought in observations and simulations by Global Climate Models (GCMs), analysing both the

## Elusive drought

B. Orlowsky and  
S. I. Seneviratne

Title Page

Abstract

Introduction

Conclusions

References

Tables

Figures

◀

▶

◀

▶

Back

Close

Full Screen / Esc

Printer-friendly Version

Interactive Discussion



magnitude and frequency of the events (Sect. 3). Potential future drought trends and their uncertainties in CMIP5 projections are analysed in Sect. 4, including an assessment of the relative uncertainty contributions of internal variability, GCM formulation and Green-House Gas (GHG) concentrations scenario to the overall projection uncertainty. A corresponding analysis is performed for a heat wave index to provide some benchmarking for the drought uncertainties. Section 5 summarises our findings and their implications.

## 2 Data, indicators and hot spots of drought

### 2.1 Data

#### 2.1.1 CMIP5

The internationally coordinated sets of CMIP5 GCM experiments provide climate simulations of past and future periods with different GHG concentrations scenarios. The ensemble constitutes one of the main data sources for the upcoming 5th Assessment Report, AR5, by the IPCC. We use monthly data from the CMIP5 *historical*, RCP2.6, RCP4.5 and RCP8.5 experiments (Moss et al., 2010), available from <http://cmip-pcmdi.llnl.gov/index.html>. The *historical* runs with observed GHG forcing finish in 2005 and the RCP experiments start in 2006, representing a peak-and-decline (RCP2.6), a stabilisation-without-overshoot (RCP4.5) and a rising (RCP8.5) GHG concentrations scenario, respectively. From each GCM, only one run is used (the r1i1p1-run if available), and only if it is available both for the *historical* and the respective RCP experiments, and if it completely covers the 1950–2100 period. Table 1 indicates the available GCM projections at the time of analysis (October 2012).

## Elusive drought

B. Orlowsky and  
S. I. Seneviratne

Title Page

Abstract

Introduction

Conclusions

References

Tables

Figures

◀

▶

◀

▶

Back

Close

Full Screen / Esc

Printer-friendly Version

Interactive Discussion



## 2.1.2 Observation-based datasets

For the comparison of observed and GCM simulated droughts, we use three global monthly precipitation datasets of different spatial resolutions, based on station observations, remote sensing data and combinations of these. We analyse the longest common period of all these datasets, 1979–2009. Observational monthly precipitation data is used from CRU TS3.1 (Climate Research Unit at the University of East Anglia, UK, Mitchell and Jones, 2005), covering 1901–2009 on a 0.5° grid; CMAP (Climate prediction center Merged Analysis of Precipitation, from the NOAA, USA, Xie and Arkin, 1997), covering 1979–2009 on a 2.5° grid, and GPCP (Global Precipitation Climatology Project, Adler et al., 2003), covering 1979–2010 on a 2.5° grid.

## 2.2 Indicators of drought and heat waves

### 2.2.1 Drought indicators

The Standardised Precipitation Index (SPI) is a commonly used indicator of meteorological drought (e.g. McKee et al., 1993; Lloyd-Hughes and Saunders, 2002; Heim, 2002; Hirschi et al., 2011; Mueller and Seneviratne, 2012; Seneviratne et al., 2012) characterising precipitation deficits or surpluses over different time scales. Here we use the 12-month time scale (SPI12) to account for long-term drought on the annual time scale, which is computed as follows. For each month, the precipitation over the preceding 12 months is summed. Then a gamma distribution is fitted to the strictly positive 12-month sums using a maximum likelihood estimation. If the estimation does not converge, the parameters of the gamma distribution are calculated using empirical relations (Lloyd-Hughes and Saunders, 2002). The last step is an equal-probability transformation to a standard normal distribution. Here, for all datasets, the gamma distribution is fitted to the monthly sums of the 1979–2009 period for a consistent comparison with the observations.

## Elusive drought

B. Orłowsky and  
S. I. Seneviratne

Title Page

Abstract

Introduction

Conclusions

References

Tables

Figures

◀

▶

◀

▶

Back

Close

Full Screen / Esc

Printer-friendly Version

Interactive Discussion



Monthly Soil Moisture Anomalies (SMAs, referring to the water content of the entire soil column) as an indicator of agricultural drought are calculated w.r.t. the 1979–2009 monthly means and standardised by the monthly 1979–2009 standard deviations. This accounts for the large spread of soil moisture variabilities in the GCMs due to different land-surface schemes, soil depths and layers, etc. (Orlowsky and Seneviratne, 2012) and ensures direct comparability with the SPI12, which is standardised over the same period.

### 2.2.2 Heat wave indicator

To put the uncertainty of drought quantification and projection into perspective, similar analyses are performed for a standard indicator of heat waves. The Warm Spell Duration Index (WSDI) counts the annual numbers of days that belong to spells of at least six days length at which the climatological 90th percentile of daily maximum temperatures is exceeded (Alexander et al., 2006; Orlowsky and Seneviratne, 2012; Sillmann et al., 2012a). The index has been calculated for the CMIP5 simulations by Sillmann et al. (2012b) and has been downloaded for our study from <ftp://ftp.cccma.ec.gc.ca/data/climdex> (October 2012).

### 2.3 Drought hot spots

For our study we identify drought hot spot regions based on impact and land use data, as well as projections of future drought changes.

The maps in Fig. 1a, b show economical and physical drought exposure for the 1980–2001 period (data provided by the United Nations Environmental Program, UNEP, at [preview.grid.unep.ch](http://preview.grid.unep.ch), last access: October 2012) as well as the global distribution of crop and pasture lands of the year 2000 (Fig. 1c, d, Monfreda et al., 2008). The maps of economical and physical exposure and the crop land distribution are very similar, and they are naturally all closely related to the population density (also available from UNEP, not shown). Correspondingly, pasture areas are found in different regions, filling

## Elusive drought

B. Orlowsky and  
S. I. Seneviratne

Title Page

Abstract

Introduction

Conclusions

References

Tables

Figures

◀

▶

◀

▶

Back

Close

Full Screen / Esc

Printer-friendly Version

Interactive Discussion



some of the gaps left by crop agriculture. Regional hot spots of drought exposure and/or intense agricultural use include Central Europe (CEU) and the Mediterranean (MED), Central North America (CNA) and Central America/Mexico (CAM), North-East Brazil (NEB), South Asia (SAS, basically India), East Asia (EAS, mostly China), the Sahel (SHE), and Eastern and Southern Africa (EAF and SAF, respectively). Australia (AUS) experienced until recently a decade-long drought (McGrath et al., 2012), not captured by the exposition data. See also Fig. 3 for the definition of the regions.

Future projections of two drought indicators in the CMIP5 ensemble, the 12-month Standardised Precipitation Index (SPI12) and Soil Moisture Anomalies (SMA, see Sect. 2 for both) show that some of these hot spots are consistently projected to become even drier during the 21st century (Fig. 1e, f displays CMIP5 ensemble averages after interpolating individual GCM patterns to a Gaussian T42 grid). This holds in particular for the Mediterranean region (MED) and Central North America (CNA). Further regions of aggravating drought include South Africa (SAF), the Amazon (AMZ) and Central America/Mexico (CAM). On the other hand, some of the drought hot spots of the recent past are projected to become wetter, e.g. East Africa (EAF), the Sahel (SHE) and India (SAS).

Note that the future drought changes from the CMIP5 projections are consistent with the projections of the preceding CMIP3 ensemble (Supplement Fig. S1; see also Orłowsky and Seneviratne, 2012; Seneviratne et al., 2012). All regions identified in this section are analysed in the remainder of the paper.

### 3 Drought changes of the recent past

#### 3.1 Robustness of global change patterns

In a recent study, Sheffield et al. (2012) computed trends in the commonly used Palmer Drought Severity Index (PDSI) using two alternative potential evaporation formulations (the Thornthwaite formulation, Thornthwaite, 1948, and the Penman-Monteith

## Elusive drought

B. Orłowsky and  
S. I. Seneviratne

Title Page

Abstract

Introduction

Conclusions

References

Tables

Figures

◀

▶

◀

▶

Back

Close

Full Screen / Esc

Printer-friendly Version

Interactive Discussion



formulation, Monteith, 1965) over the 1950–2008 period, derived from an observation-based dataset. It finds several regions of significantly increased drought with both potential evapotranspiration formulations, most notably in East Asia, Central and Sahelian Africa, Central and Southern Europe and Eastern Australia. These regional results also agree with the recent study by Dai (2012), although the two studies do not agree regarding trends in the global area affected by drought (Sheffield et al., 2012; Seneviratne, 2012). Here we complement the analyses of Sheffield et al. (2012) and Dai (2012) by assessing the robustness of trends in CMIP5 simulations of SPI12 and SMA over two periods, 1950–2009 and 1979–2009. For the latter and SPI12, trends from the three observational precipitation datasets CRU, CMAP and GPCP (Sect. 2) are included in the analysis. We assess trends from linear least-squares regression of annual averages of SPI12 and SMA against time and evaluate the statistical significance of the trend being different from zero by the standard t-test at the 5 %-significance level. Note that this interpretation of significance may be not stringent enough w.r.t. detecting significant trends, due to auto-correlation in the time series. Trend and p-values of the linear regression on the original GCM grids are interpolated to a common 0.5° grid by nearest-neighbour assignment prior to the assessment of agreeing significant trends.

Figure 2 assesses the agreement on drought trends in the historical CMIP5 simulations (the years after 2005 are taken from the continuing runs into the RCP8.5 GHG concentrations scenario). For SPI12, the only extended land region of rather consistent trends are the Northern high latitudes, where approximately half of the 32 GCMs indicate significant positive trends (Fig. 2a, c). This is further supported by the relatively consistent increases in the observational datasets (Fig. 2c). The observational trends roughly follow a pattern of wetting high latitudes, neutral trends in mid-latitudes, drying in the sub tropics and wetting in the tropics, although only few regions show consistent trends in all three datasets. Note that this pattern only partially agrees with the trend pattern found from zonal averaged precipitation anomalies in Zhang et al. (2007), for example their drying (wetting) trends just north (south) of the equator are the opposite of what we find. Furthermore, in particular over parts of Eastern Asia and Africa the

**Elusive drought**B. Orlowsky and  
S. I. Seneviratne

Title Page

Abstract

Introduction

Conclusions

References

Tables

Figures

◀

▶

◀

▶

Back

Close

Full Screen / Esc

Printer-friendly Version

Interactive Discussion



patterns of increase or decrease do not depend on latitude only, limiting the value of the zonal average for that regional scale. Finally, the observed pattern is not reproduced in the CMIP5 ensemble.

Overall, especially for the 1979–2009 period in Fig. 2c, d the CMIP5 patterns are dominated either by consistently no significant trends (white) or by contradicting signals (grey shading), which holds in particular for SMA, where only a few scattered patches show consistent drying trends in the CMIP5 simulations. Furthermore, for both indicators consistent trends are only found in rather small subsets of the CMIP5 ensemble. We conclude that the detection of drought hot spots from trends in the observational period remains a significant challenge.

### 3.2 Past changes of drought in selected hot spot regions

In the remainder of this article, we present results from analysing the drought hot spots identified in Sect. 2. Given the many severe drought events in the last years, e.g. the “Texas” drought in Southern US and Mexico since 2010 (regions Central North America, CNA, and Central America/Mexico, CAM), the drought at the Horn of Africa in 2011 (region East Africa, EAF) and the China droughts 2009–2011 (region East Asia, EAS), obvious questions are whether these events are exceptional or within internal climate variability, whether drought magnitude or frequency has increased or decreased over the last decades, and whether there will be such trends in the future.

Figure 3 displays time series of SPI12 from three observational datasets, averaged with grid cell area weighting over the land grid cells with centres in the identified hot spot regions. Shading indicates the range of the corresponding CMIP5 time series of the same regions and period. The conclusions for the recent past of all investigated regions are very similar. First, the three observational datasets correlate reasonably well, although the amplitudes are less consistent. Second, there are no trends over this period, neither in the observations nor in the GCM ensemble (see also Fig. 2). Global trends towards increased dryness as found in Dai (2012) for the last decades are not reproduced by the SPI12 at this regional scale. Last, the dry years depicted

## Elusive drought

B. Orlowsky and  
S. I. Seneviratne

Title Page

Abstract

Introduction

Conclusions

References

Tables

Figures

◀

▶

◀

▶

Back

Close

Full Screen / Esc

Printer-friendly Version

Interactive Discussion



**Elusive drought**B. Orlowsky and  
S. I. Seneviratne[Title Page](#)[Abstract](#)[Introduction](#)[Conclusions](#)[References](#)[Tables](#)[Figures](#)[I◀](#)[▶I](#)[◀](#)[▶](#)[Back](#)[Close](#)[Full Screen / Esc](#)[Printer-friendly Version](#)[Interactive Discussion](#)

by the SPI12 in the observational data always fall within the range of the GCM ensemble. Using that range as an estimate of internal climate variability (which seems reasonable, since no effect of greenhouse gas forcing is apparent in the GCM ensemble simulations and is therefore, if existent at all, much smaller than internal variability), the observed droughts are not exceptional, despite their sometimes devastating societal and economical effects. A complementary analysis of the occurrence frequencies of months with SPI12 below  $-0.5$  in moving 10-yr windows (representing only mild drought conditions, see Lloyd-Hughes and Saunders, 2002) is presented in Fig. 4. The obtained conclusions are basically the same as for the SPI12 magnitude. Only for the Mediterranean the GCM simulations seem to indicate increased drought, although this is not consistently found in the observations. The volatility in some of the observational frequency series is due to the sometimes very few SPI12 values lying below  $-0.5$ .

The corresponding analysis for SMA in the CMIP5 simulations (Figs. 5 and 6) displays more consistent tendencies, in particular for the frequencies of months with SMA below  $-0.5$  standard deviations rather than SMA itself (see the MED, CAM, AMZ, NEB and SAF panels in Fig. 6 for increasing drought). Our analysis thus indicates that the drying in these regions is not due to decreases in (standardised) precipitation, but is linked to the effect of increased evapotranspiration (and/or runoff), which can drive soil drying even if precipitation does not change (Seneviratne, 2012). The higher consistency for frequencies compared to magnitude may be related to physical limits of the system. For example, if a soil approaches dry-out, SMA cannot decrease any further, while the frequency of SMA below some threshold can still increase. However, both for magnitudes and frequencies and in all investigated regions, uncertainty is larger than the changes over the period. This finding agrees with Fig. 2, which indicates large uncertainty on SMA trends across the CMIP5 ensemble. The few spots of systematic SMA decreases in Fig. 2 are consistent with the drying regions identified in Fig. 6.

Time series of top-layer soil moisture from a merged active and passive micro-wave remote sensing dataset (Liu et al., 2012) display an unrealistic interannual variability (not shown) and are compromised by instrumentation changes over time. They are

therefore omitted from our analyses. In the absence of any other reliable observation based soil moisture dataset with global coverage (Seneviratne et al., 2010), a comparison between observed SMA and GCM simulations and their internal variability is not feasible.

## 4 Drought changes in future projections

### 4.1 Future changes of drought in selected hot spot regions

In Fig. 7, we show future drought projections for six of the twelve hot spot regions. They have in common that SPI12 increases (Fig. 7a), with the clearest signals in the Asian and African regions (except for Sahel), some of them present-day drought hot spots (e.g. EAF, SAS and EAS, see Sect. 2). For these regions there is also a clear dependence on the GHG concentrations scenario, with the stronger scenarios coinciding with stronger changes. In contrast, the US and Europe have weaker signals. Soil Moisture Anomalies (SMA, see Fig. 7b) show generally more uncertainty, with trends of unclear sign and a much larger GCM-ensemble spread, which includes both substantial in- and decreases of soil moisture. On average, the small changes of soil moisture indicate compensating effects of increased evaporation and/or runoff which offset the increases in precipitation. Central North America (CNA) and Central Europe (CEU) even suggest slight decreases of soil moisture, hinting at a stronger increase of evapotranspiration than precipitation decrease in these regions.

In the remaining six hot spot regions, SPI12 decreases to varying degrees (Fig. 8a), and soil moisture decreases accordingly (Fig. 8c). The Mediterranean (MED) displays the clearest decrease, followed by South Africa (SAF) and Central America/Mexico (CAM). These trends are even more visible when frequencies rather than magnitudes of drought are analysed, as Fig. 8b, d shows by the number of months per year in which the SPI12 and SMA drop below  $-1$ , calculated for moving 10-yr windows. SPI12-values below  $-1$  indicate at least “moderate drought” (see e.g. Lloyd-Hughes and Saunders,

## Elusive drought

B. Orłowsky and  
S. I. Seneviratne

Title Page

Abstract

Introduction

Conclusions

References

Tables

Figures

◀

▶

◀

▶

Back

Close

Full Screen / Esc

Printer-friendly Version

Interactive Discussion



2002), while SMA below  $-1$  indicates one standard deviation below normal w.r.t. to the 1979–2009 period (see Sect. 2). For most regions both magnitude and frequency projections show large uncertainties, the range often allowing for negative as well as positive trends.

## 5 4.2 Sources of uncertainty in drought projections

To investigate the causes behind the large uncertainty in drought projections, we separate the total uncertainty of the CMIP5 ensemble into contributions from internal variability, GCM formulation and GHG concentrations scenarios. To this end we apply a modified version of the method proposed in Hawkins and Sutton (2009, see Fig. 9), using all available projections in the CMIP5 ensemble (as of October 2012) from the RCP2.6, RCP4.5 and RCP8.5 experiments. In a preparatory step, a 4th order polynomial is fitted to the annual values (e.g. annual average SMA) of each GCM simulated time series using least squares regression (Fig. 9a) to identify the long-term trend component of the time series. From this,

- the time-independent internal variability,  $V$ , is defined as the multi-GCM and multi-scenario average over the variances of the residuals of the polynomial fit of each GCM series (Fig. 9a),
- the GCM or model uncertainty of a given year  $t$ ,  $M_t$ , is the average over all GHG concentrations scenarios of the within-scenario variances of the fitted polynomials at year  $t$  (Fig. 9b),
- and the scenario uncertainty of a given year  $t$ ,  $S_t$ , is the variance of the multi-GCM means of each scenario (Fig. 9b) at year  $t$ .

We use equal weights for all GCMs.

By construction, the total variance of the entire ensemble at a given year  $t$  equals the sum of the three uncertainty contributions,  $T_t = V + M_t + S_t$  and its square root  $\sqrt{T_t}$  defines the total uncertainty. The fractional uncertainty,  $F_t$ , of a future year  $t$  is defined

## Elusive drought

B. Orlowsky and  
S. I. Seneviratne

Title Page

Abstract

Introduction

Conclusions

References

Tables

Figures

◀

▶

◀

▶

Back

Close

Full Screen / Esc

Printer-friendly Version

Interactive Discussion



## Elusive drought

B. Orlowsky and  
S. I. Seneviratne

Title Page

Abstract

Introduction

Conclusions

References

Tables

Figures

◀

▶

◀

▶

Back

Close

Full Screen / Esc

Printer-friendly Version

Interactive Discussion



as the total uncertainty  $\sqrt{T_t}$  divided by the change between that future year and a reference year,  $G_t$ , calculated from the average of the fitted polynomials of all GCMs and all scenarios of that year (Fig. 9c). If this ratio  $F_t = \sqrt{T_t}/G_t$  drops below the value of one, the change signal is larger than the uncertainty and thus detectable. Note that Hawkins and Sutton (2009) use the more restrictive 90% confidence interval (approximately  $1.65\sqrt{T_t}$ ) instead of the standard deviation ( $\sqrt{T_t}$ ).

Figure 10 presents the results of this analysis for the same regions as in Fig. 8 (those with decreasing SPI12) for the drought indicators SPI12 and SMA (together with their frequency time series of months with values below  $-1$ ) and the heat wave indicator WSDI for reference. The panels show the total fractional uncertainty,  $F_t = \sqrt{T_t}/G_t$ , w.r.t. the reference year 2006, with the topmost black curve. The area beneath is shaded according to the relative uncertainty contributions from the GCMs' formulation ( $M_t/G_t$ , blue), internal variability ( $V/G_t$ , orange), and scenario uncertainty ( $S_t/G_t$ , green).

The projections of SPI12 and SMA (Fig. 10, first and third columns) never reach the critical detection threshold, irrespective of the region. The frequency of drought series according to SPI12 (analysed in the second column) come closer to the detection threshold compared to the SPI12 series itself but do not cross it either. Only for frequency of drought series according to SMA (fourth column) and for the Mediterranean, South Africa and Central America/Mexico regions, a detectable change signal is found. Furthermore, scenario uncertainty plays only a minor role and can in most cases be neglected in relation to internal variability and GCM uncertainty. For the meteorological drought indicator SPI12, internal variability remains an important (and often the dominant) uncertainty contributor until 2100. In contrast, for projections of agricultural drought (SMA) uncertainty is only dominated by internal variability over the very first years, while GCM uncertainty becomes strongly dominant after approximately 2030.

These findings stand in clear opposition to the heat wave projections, for which GCM formulation never contributes significantly to the total uncertainty (last column in Fig. 10). After a short period in which internal variability constitutes the dominant source of uncertainty, total fractional uncertainty drops below 1 no later than 2030 in

all regions, and thereafter the clear dominant source of uncertainty is the GHG concentrations scenario. In fact, if one chose, as history will do, one GHG concentrations scenario and thus subtracted the GHG concentrations scenario contribution from the total fractional uncertainty, projected changes of heat waves for the end of the 21st century (which increase, not shown) would be extremely consistent across the GCMs, while the uncertainty of drought would be reduced much less.

## 5 Conclusions

Droughts constitute one of the most societal relevant weather and climate phenomena, and recent years have seen a particularly high impact from drought. However, our analysis of the 12-month Standardised Precipitation Index (SPI12) indicates that the recent droughts are not exceptional in a climatological sense but are consistent with the range of internal climate variability estimated from the CMIP5 ensemble of GCM simulations. Regional SPI12 series of drought hot-spots show no trend over the last decades in observations and CMIP5 simulations, but Soil Moisture Anomalies (SMA) from CMIP5 as a measure of agricultural drought suggest increasing drought in some regions, most importantly in the Mediterranean. Increases in agricultural drought during the recent past are therefore not driven by decreased precipitation but by increased evapotranspiration and/or runoff, questioning the value of the SPI as a measure of drought. The increase is more evident for drought frequencies than magnitudes of the indicators. Although the CMIP5 ensemble displays a consistent increase of agricultural drought for several regions in recent decades, the overall uncertainty of these changes is large and in particular much larger than the signals themselves. Only very few GCMs, and only over very limited areas, show consistent statistically significant trends for the last decades.

Large internal variability and general uncertainty is also found in future GCM projections until the end of the 21st century, generally inhibiting a robust trend detection in many areas. This holds both for meteorological drought (as quantified by the SPI12)

### Elusive drought

B. Orlowsky and  
S. I. Seneviratne

Title Page

Abstract

Introduction

Conclusions

References

Tables

Figures

◀

▶

◀

▶

Back

Close

Full Screen / Esc

Printer-friendly Version

Interactive Discussion



and agricultural drought (measured by SMA). The signals are stronger in the SMA projections compared to SPI12, since SMAs integrate effects of increased evaporation and/or runoff in the course of global warming in addition to potential changes in precipitation. However, even for these regions the changes in the drought indicators themselves are at best of the order of magnitude of the overall uncertainty in the CMIP5 ensemble. Only for agricultural drought and for frequencies rather than magnitudes, the changes become larger than the overall ensemble uncertainty in a few regions, namely the Mediterranean, South Africa and Central America/Mexico.

Drought hot spot regions of the last decades such as the Sahel, East Africa or South Asia are projected to become less drought-prone, although the uncertainties remain large. In some regions, e.g. Central Europe, East Asia or Australia, drought projections range between strong drying and wetting conditions. Extreme drying scenarios are therefore about as likely as significantly reduced drought risk.

Partitioning the overall ensemble uncertainty of future drought projections into contributions from internal variability, GCM formulation and GHG concentrations scenario uncertainty shows large contributions from internal variability for the next decades, especially for SPI12. This indicates that there is only limited potential to decrease the uncertainty of meteorological drought projections. On the other hand, the overall uncertainty for SMA is dominated by uncertainty from GCM formulation already in the near future, which highlights the known uncertainty in the representation of land-surface processes in the GCMs (Koster et al., 2004; Sheffield and Wood, 2008; Seneviratne et al., 2010). GHG concentrations scenario uncertainty hardly contributes to overall drought uncertainty, except for the SPI12 in the Mediterranean. These findings stand in contrast with those for projections of heat waves, for which GHG concentrations scenarios constitute the main source of uncertainty and which show detectable changes already after approximately 2030 in all analysed regions.

In summary, our results emphasise the large uncertainty in the quantification and projection of drought on the regional scale. However, the large uncertainty range must not be mistaken for low drought risk, since projections for all regions include the

## Elusive drought

B. Orłowsky and  
S. I. Seneviratne

Title Page

Abstract

Introduction

Conclusions

References

Tables

Figures

◀

▶

◀

▶

Back

Close

Full Screen / Esc

Printer-friendly Version

Interactive Discussion



possibility of increasing drought, even in cases where the average projections point towards wetter conditions. This is particularly critical as some of these regions are vital for global food production.

**Supplementary material related to this article is available online at:**  
<http://www.hydrol-earth-syst-sci-discuss.net/9/13773/2012/hessd-9-13773-2012-supplement.pdf>.

*Acknowledgements.* We acknowledge the World Climate Research Programme's Working Group on Coupled Modelling, which is responsible for CMIP, and we thank the climate modelling groups for producing and making available their model output. For CMIP the US Department of Energy's Program for Climate Model Diagnosis and Intercomparison provides coordinating support and led development of software infrastructure in partnership with the Global Organization for Earth System Science Portals. We also thank Urs Beyerle and Thierry Corti (C2SM) for support with the downloading and storage of the CMIP5 data. We are grateful to the ETCCDI team at the Canadian Center for Climate Modelling and Analysis for computing and making available the heat wave indicator WSDI. We acknowledge partial funding from the EU 7th framework program through the DROUGHT-RSPI and EMBRACE projects.

## References

- Adler, R. F., Huffman, G. J., Chang, A., Ferraro, R., Xie, P. P., Janowiak, J., Rudolf, B., Schneider, U., Curtis, S., Bolvin, D., Gruber, A., Susskind, J., Arkin, P., and Nelkin, E.: The version 2 global precipitation climatology project (GPCP) monthly precipitation analysis (1979–present), *J. Hydrometeorol.*, 4, 1147–1167, 2003. 13777
- Alexander, L., Zhang, X., Peterson, T., Caesar, J., Gleason, B., Tank, A., Haylock, M., Collins, D., Trewin, B., Rahimzadeh, F., Tagipour, A., Kumar, K., Revadekar, J., Griffiths, G., Vincent, L., Stephenson, D., Burn, J., Aguilar, E., Brunet, M., Taylor, M., New, M., Zhai, P., Rusticucci, M., and Vazquez-Aguirre, J.: Global observed changes in daily climate extremes of temperature and precipitation, *J. Geophys. Res.*, 111, D05109, doi:10.1029/2005JD006290, 2006. 13778

13788

**HESSD**

9, 13773–13803, 2012

## Elusive drought

B. Orlowsky and  
S. I. Seneviratne

Title Page

Abstract

Introduction

Conclusions

References

Tables

Figures

◀

▶

◀

▶

Back

Close

Full Screen / Esc

Printer-friendly Version

Interactive Discussion



- Barriopedro, D., Gouveia, C. M., Trigo, R. M., and Wang, L.: The 2009/10 Drought in China: Possible Causes and Impacts on Vegetation, *J. Hydrometeorol.*, 13, 1251–1267, doi:10.1175/JHM-D-11-074.1, 2012. 13775
- Dai, A.: Increasing drought under global warming in observations and models, *Nature Clim. Change*, doi:10.1038/nclimate1633, in press, 2012. 13780, 13781
- Foley, J. A., Ramankutty, N., Brauman, K. A., Cassidy, E. S., Gerber, J. S., Johnston, M., Mueller, N. D., O'Connell, C., Ray, D. K., West, P. C., Balzer, C., Bennett, E. M., Carpenter, S. R., Hill, J., Monfreda, C., Polasky, S., Rockstrom, J., Sheehan, J., Siebert, S., Tilman, D., and Zaks, D. P. M.: Solutions for a cultivated planet, *Nature*, 478, 337–342, doi:10.1038/nature10452, 2011. 13775
- Friedlingstein, P., Cox, P., Betts, R., Bopp, L., Bloh, W. V., Brovkin, V., Cadule, P., Doney, S., Eby, M., Fung, I., Bala, G., John, J., Jones, C., Joos, F., Kato, T., Kawamiya, M., Knorr, W., Lindsay, K., Matthews, H. D., Raddatz, T., Rayner, P., Reick, C., Roeckner, E., Schnitzler, K. G., Schnur, R., Strassmann, K., Weaver, A. J., Yoshikawa, C., and Zeng, N.: Climate-carbon cycle feedback analysis: results from the CMIP model intercomparison, *J. Climate*, 19, 3337–3353, 2006. 13775
- Hawkins, E. and Sutton, R.: The potential to narrow uncertainty in regional climate predictions, *B. Am. Meteorol. Soc.*, 90, 1095–1107, 2009. 13784, 13785, 13802
- Heim, R.: A review of twentieth-century drought indices used in the United States, *B. Am. Meteorol. Soc.*, 83, 1149–1166, 2002. 13777
- Hirschi, M., Seneviratne, S. I., Alexandrov, V., Boberg, F., Boroneant, C., Christensen, O. B., Formayer, H., Orlowsky, B., and Stepanek, P.: Observational evidence for soil-moisture impact on hot extremes in southeastern Europe, *Nat. Geosci.*, 4, 17–21, doi:10.1038/ngeo1032, 2011. 13777
- Hoerling, M., Kumar, A., Dole, R., Nielsen-Gammon, J. W., Eischeid, J., Perlwitz, J., Quan, X.-W., Zhang, T., Pegion, P., and Chen, M.: Anatomy of an extreme event, *J. Climate*, doi:10.1175/JCLI-D-12-00270.1, in press, 2012. 13775
- IPCC: Managing the Risks of Extreme Events and Disasters to Advance Climate Change Adaptation. A Special Report of Working Groups I and II of the Intergovernmental Panel on Climate Change, edited by: Field, C. B., Barros, V., Stocker, T. F., Qin, D., Dokken, D. J., Ebi, K. L., Mastrandrea, M. D., Mach, K. J., Plattner, G.-K., Allen, S. K., Tignor, M., and Midgley, P. M., Cambridge University Press, Cambridge, UK, and New York, NY, USA, 2012. 13775

**Elusive drought**B. Orlowsky and  
S. I. Seneviratne

Title Page

Abstract

Introduction

Conclusions

References

Tables

Figures

◀

▶

◀

▶

Back

Close

Full Screen / Esc

Printer-friendly Version

Interactive Discussion



**Elusive drought**B. Orlowsky and  
S. I. Seneviratne

Title Page

Abstract

Introduction

Conclusions

References

Tables

Figures

◀

▶

◀

▶

Back

Close

Full Screen / Esc

Printer-friendly Version

Interactive Discussion



- Koster, R. D., Suarez, M. J., Liu, P., U, U. J., Berg, A., Kistler, M., Reichle, R., Rodell, M., and Famiglietti, J.: Realistic initialization of land surface states: impacts on subseasonal forecast skill, *J. Hydrometeorol.*, 5, 1049–1063, 2004. 13787
- Lenton, T., Held, H., Kriegler, E., Hall, J., Lucht, W., Rahmstorf, S., and Schellnhuber, H.: Tipping elements in the Earth's climate system, *Proc. Natl. Acad. Sci.*, 105, 1786–1793, 2008. 13775
- Lewis, S., Brando, P., Phillips, O., van der Heijden, G., and Nepstad, D.: The 2010 Amazon drought, *Science*, 331, 554–554, 2011. 13775
- Liu, Y. Y., Dorigo, W. A., Parinussa, R. M., de Jeu, R. A. M., Wagner, W., McCabe, M. F., Evans, J., and van Dijk, A.: Trend-preserving blending of passive and active microwave soil moisture retrievals, *Remote Sens. Environ.*, 123, 280–297, 2012. 13782
- Lloyd-Hughes, B. and Saunders, M.: A drought climatology for Europe, *Int. J. Climatol.*, 22, 1571–1592, 2002. 13777, 13782, 13783
- Lyon, B. and DeWitt, D. G.: A recent and abrupt decline in the East African long rains, *Geophys. Res. Lett.*, 39, L02 702, doi:10.1029/2011GL050337, 2012. 13775
- Marengo, J., Nobre, C., Tomasella, J., Oyama, M., Sampaio de Oliveira, G., de Oliveira, R., Camargo, H., Alves, L., and Brown, I.: The drought of Amazonia in 2005, *J. Climate*, 21, 495–516, 2008. 13775
- McGrath, G. S., Sadler, R., Fleming, K., Tregoning, P., Hinz, C., and Veneklaas, E. J.: Tropical cyclones and the ecohydrology of Australia's recent continental-scale drought, *Geophys. Res. Lett.*, 39, L03404, doi:10.1029/2011GL050263, 2012. 13775, 13779
- McKee, T. B., Oeskin, N. J. D., and Kleist, J. K.: The relationship of drought frequency and duration to time scales, in: 8th Conference on Applied Climatology, American Meteorological Society, Anaheim, Canada, 179–184, 1993. 13777
- Mitchell, T. and Jones, P.: An improved method of constructing a database of monthly climate observations and associated high-resolution grids, *Int. J. Climatol.*, 25, 693–712, 2005. 13777
- Monfreda, C., Ramankutty, N., and Foley, J.: Farming the planet: 2. geographic distribution of crop areas, yields, physiological types, and net primary production in the year 2000, *Global Biogeochem. Cy.*, 22, 1–19, 2008. 13775, 13778
- Monteith, J.: Evaporation and environment, *Symp. Soc. Exp. Biol.*, 19, 205–234, 1965. 13780
- Moss, R. H., Edmonds, J. A., Hibbard, K. A., Manning, M. R., Rose, S. K., van Vuuren, D. P., Carter, T. R., Emori, S., Kainuma, M., Kram, T., Meehl, G. A., Mitchell, J. F. B., Nakicenovic,

**Elusive drought**B. Orlowsky and  
S. I. Seneviratne

Title Page

Abstract

Introduction

Conclusions

References

Tables

Figures

◀

▶

◀

▶

Back

Close

Full Screen / Esc

Printer-friendly Version

Interactive Discussion



N., Riahi, K., Smith, S. J., Stouffer, R. J., Thomson, A. M., Weyant J. P., and Wilbanks, T. J.: The next generation of scenarios for climate change research and assessment, *Nature*, 463, 747–756, 2010. 13776

Mueller, B. and Seneviratne, S.: Hot days induced by precipitation deficits at the global scale, *Proc. Natl. Acad. Sci.*, 109, 12398–12403, 2012. 13777

Orlowsky, B. and Seneviratne, S. I.: Global changes in extreme events: Regional and seasonal dimension, *Clim. Change*, 110, 669–696, 2012. 13778, 13779

Peterson, T., Stott, P., and Herring, S.: Explaining extreme events of 2011 from a climate perspective, *B. Am. Meteorol. Soc.*, 93, 1041–1067, 2012. 13775

Poulter, B., Hattermann, F., Hawkins, E., Zaehle, S., Sitch, S., Restrepo-Coupe, N., Heyder, U., and Cramer, W.: Robust dynamics of Amazon dieback to climate change with perturbed ecosystem model parameters, *Global Biogeochem. Cy.*, 16, 2476–2495, doi:10.1111/j.1365-2486.2009.02157.x, 2010. 13775

Seneviratne, S. I.: Climate science: historical drought trends revisited, *Nature*, 491, 338–339, doi:10.1038/491338a, 2012. 13775, 13780, 13782

Seneviratne, S. I., Corti, T., Davin, E. L., Jaeger, E. B., Hirschi, M., Lehner, I., Orlowsky, B., and Teuling, A. J.: Investigating soil moisture-climate interactions in a changing climate: a review, *Earth-Sci. Rev.*, 99, 125–161, 2010. 13783, 13787

Seneviratne, S. I., Nicholls, N., Easterling, D., Goodess, C., Kanae, S., Kossin, J., Luo, Y., Marengo, J., McInnes, K., Rahimi, M., Reichstein, M., Sorteberg, A., Vera, C., and Zhang, X.: Changes in climate extremes and their impacts on the natural physical environment, in: *Managing the Risks of Extreme Events and Disasters to Advance Climate Change Adaptation. A Special Report of Working Groups I and II of the Intergovernmental Panel on Climate Change (IPCC)*, edited by: Field, C. B., Barros, V., Stocker, T., Qin, D., Dokken, D., Ebi, K., Mastrandrea, M., Mach, K., Plattner, G.-K., Allen, S., Tignor, M., and Midgley, P., Cambridge University Press, Cambridge, UK, and New York, NY, USA, 109–230, 2012. 13775, 13777, 13779

Sheffield, J. and Wood, E.: Projected changes in drought occurrence under future global warming from multi-model, multi-scenario, IPCC AR4 simulations, *Clim. Dynam.*, 31, 79–105, doi:10.1007/s00382-007-0340-z, 2008. 13787

Sheffield, J., Wood, E. F., and Roderick, M. L.: Little change in global drought over the past 60 years, *Nature*, 491, 435–438, doi:10.1038/nature11575, 2012. 13779, 13780

**Elusive drought**B. Orlowsky and  
S. I. Seneviratne

Title Page

Abstract

Introduction

Conclusions

References

Tables

Figures

I◀

▶I

◀

▶

Back

Close

Full Screen / Esc

Printer-friendly Version

Interactive Discussion



- Sillmann, J., Kharin, V. V., Zwiers, F. W., and Zhang, X.: Climate extreme indices in the CMIP5 multi-model ensemble, Pt. 1: model evaluation in the present climate, *J. Geophys. Res.*, submitted, 2012a. 13778
- 5 Sillmann, J., Kharin, V. V., Zwiers, F. W., and Zhang, X.: Climate extreme indices in the CMIP5 multi-model ensemble, Pt. 2: future climate projections, *J. Geophys. Res.*, submitted, 2012b. 13778
- Sun, C. and Yang, S.: Persistent severe drought in southern China during winter and spring 2011: Large-scale circulation patterns and possible impacting factors, *J. Geophys. Res.*, 117, D10112, doi:10.1029/2012JD017500, 2012. 13775
- 10 Thornthwaite, C. W.: An approach toward a rational classification of climate, *Geogr. Rev.*, 38, 55–94, 1948. 13779
- Xie, P. and Arkin, P.: Global precipitation: a 17-year monthly analysis based on gauge observations, satellite estimates, and numerical model outputs, *B. Am. Meteorol. Soc.*, 78, 2539–2558, 1997. 13777
- 15 Zhang, X., Zwiers, F., Hegerl, G., Lambert, F., Gillett, N., Solomon, S., Stott, P., and Nozawa, T.: Detection of human influence on twentieth-century precipitation trends, *Nature*, 448, 461–465, 2007. 13780

**Table 1.** GCMs from the CMIP5 used in our study. Columns give GCM name, horizontal resolution and for each future GHG concentrations scenario the drought and heat wave indicators that could be calculated from each GCM.

GCM	Resolution	RCP2.6	RCP4.5	RCP8.5
BCC-CSM1.1	Gaussian 128 × 64	SPI,SMA	SPI,SMA	SPI,SMA,CDD
BCC-CSM1.1(m)	Gaussian 320 × 160	SPI	SPI,SMA	CDD
CanESM2	Gaussian 128 × 64	SPI,SMA,WSDI	SPI,SMA,WSDI	SPI,SMA,CDD,WSDI
CMCC-CESM	Gaussian 96 × 48			CDD
CMCC-CM	Gaussian 480 × 240		SPI,SMA,WSDI	SPI,SMA,WSDI
CMCC-CMS	Gaussian 192 × 96		SPI,SMA	SPI,SMA,CDD
CNRM-CM5	Gaussian 256 × 128	SPI,SMA,WSDI	SPI,SMA,WSDI	SPI,SMA,CDD,WSDI
ACCESS1.0	192 × 145		SPI,SMA,WSDI	SPI,SMA,CDD,WSDI
ACCESS1.3	192 × 145		SPI,SMA	SPI,SMA,CDD
CSIRO-Mk3.6.0	Gaussian 192 × 96	SPI,SMA,WSDI	SPI,SMA,WSDI	SPI,SMA,CDD,WSDI
EC-EARTH	Gaussian 320 × 160	SPI	WSDI	SPI,CDD
FIO-ESM	Gaussian 128 × 64	SPI	SPI	SPI
BNU-ESM	Gaussian 128 × 64	SPI,SMA,WSDI	SPI,SMA,WSDI	SPI,SMA,CDD,WSDI
INM-CM4	180 × 120		SPI,SMA,WSDI	SPI,SMA,CDD,WSDI
IPSL-CM5A-LR	96 × 96	SPI,SMA,WSDI	SPI,SMA,WSDI	SPI,SMA,CDD,WSDI
IPSL-CM5A-MR	144 × 143	SPI,SMA,WSDI	SPI,SMA,WSDI	SPI,SMA,CDD,WSDI
IPSL-CM5B-LR	96 × 96		WSDI	WSDI
FGOALS-g2	128 × 60	SPI,SMA	SPI,SMA	SPI,SMA,CDD
FGOALS-s2	Gaussian 128 × 108	SPI,SMA,WSDI	SPI,SMA,WSDI	SPI,SMA,CDD,WSDI
MIROC5	Gaussian 256 × 128	SPI,SMA,WSDI	SPI,SMA,WSDI	SPI,SMA,CDD,WSDI
MIROC-ESM	Gaussian 128 × 64	SPI,SMA,WSDI	SPI,SMA,WSDI	SPI,SMA,CDD,WSDI
MIROC-ESM-CHEM	Gaussian 128 × 64	SPI,SMA,WSDI	SPI,SMA,WSDI	SPI,SMA,CDD,WSDI
HadGEM2-CC	192 × 145			CDD
HadGEM2-ES	192 × 145	WSDI	WSDI	CDD
MPI-ESM-LR	Gaussian 192 × 96	SPI,SMA,WSDI	SPI,SMA,WSDI	SPI,SMA,CDD,WSDI
MPI-ESM-MR	Gaussian 192 × 96	SPI,SMA,WSDI	SPI,SMA,WSDI	SPI,SMA,CDD,WSDI
MRI-CGCM3	Gaussian 320 × 160	SPI,SMA,WSDI	SPI,SMA,WSDI	SPI,SMA,CDD,WSDI
GISS-E2-H-CC	144 × 90		SPI,SMA	SPI,SMA
GISS-E2-R	144 × 90	SPI,SMA	SPI,SMA,WSDI	SPI,SMA
GISS-E2-R-CC	144 × 90		SPI,SMA	
CCSM4	288 × 192	SPI,SMA	SPI,SMA	SPI,SMA,CDD
NorESM1-M	144 × 96	SPI,SMA,WSDI	SPI,SMA,WSDI	SPI,SMA,CDD,WSDI
NorESM1-ME	144 × 96	SPI,SMA	SPI,SMA	SPI,SMA
HadGEM2-AO	192 × 145	SPI	SPI	SPI
GFDL-CM3	144 × 90	SPI,WSDI	SPI	SPI,CDD,WSDI
GFDL-ESM2G	144 × 90	SPI,SMA,WSDI	SPI,SMA,WSDI	SPI,SMA,CDD,WSDI
GFDL-ESM2M	144 × 90	SPI,SMA,WSDI	SPI,SMA,WSDI	SPI,SMA,CDD,WSDI
CESM1(BGC)	288 × 192		SPI,SMA,WSDI	SPI,SMA,CDD,WSDI
CESM1(CAM5)	288 × 192	SPI	SPI	SPI,SMA

## Elusive drought

B. Orłowsky and  
S. I. Seneviratne

Title Page

Abstract

Introduction

Conclusions

References

Tables

Figures

◀

▶

◀

▶

Back

Close

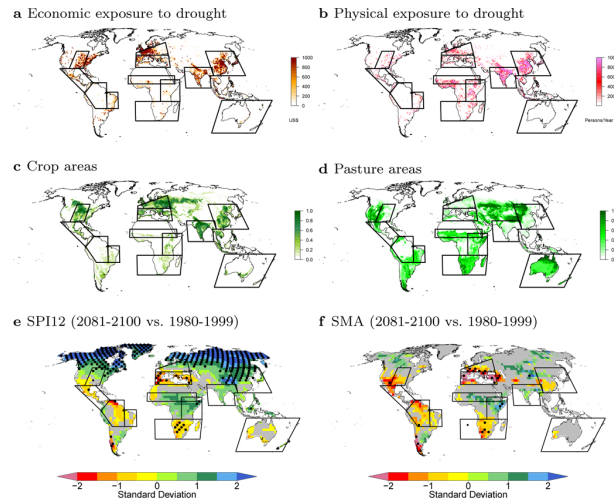
Full Screen / Esc

Printer-friendly Version

Interactive Discussion



## Elusive drought

B. Orlowsky and  
S. I. Seneviratne

**Fig. 1.** Exposure to drought, land uses and future changes of drought in CMIP5 projections. **(a)** Economic exposure to drought in 1980–2001 measured by the expected average annual Gross Domestic Product GDP (2007 as the year of reference) exposed to drought (in US\$, year 2000 equivalent). **(b)** Physical exposure to drought measured by the number of persons exposed to drought per year over 1980–2001. **(c)** Crop areas as grid cell percentages for the year 2000. **(d)** Pasture areas as grid cell percentages for the year 2000. **(e)** Multi-GCM averages of multi-year average changes in 12-month Standardised Precipitation Index (SPI12) between present-day (1980–1999) and future (2081–2100), divided by the standard deviation of detrended annual values. The GCM projections are based on the RCP8.5 GHG concentrations scenario. **(f)** As **(e)**, but for changes in average Soil Moisture Anomalies (SMA). Colour shading in **(e)** and **(f)** indicates at least 66 % of the GCMs agreeing on the sign of change, additional stippling (black dots) indicates 90 % agreement. Gray shading indicates less than 66 % GCM agreement on the sign, and if stippled (black diamonds), consistent small changes (at least 66 % of the GCMs display changes smaller than half a standard deviation). Increased drought is indicated with yellow-red shading. Outlined regions in all maps indicate the hot spots that are analysed in our study.

Title Page

Abstract

Introduction

Conclusions

References

Tables

Figures

◀

▶

◀

▶

Back

Close

Full Screen / Esc

Printer-friendly Version

Interactive Discussion



## Elusive drought

B. Orlowsky and  
S. I. Seneviratne

Title Page

Abstract

Introduction

Conclusions

References

Tables

Figures

◀

▶

◀

▶

Back

Close

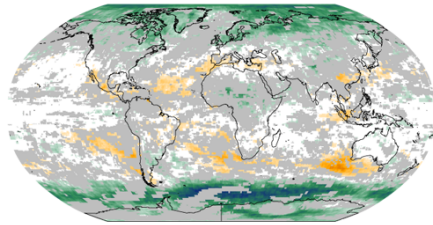
Full Screen / Esc

Printer-friendly Version

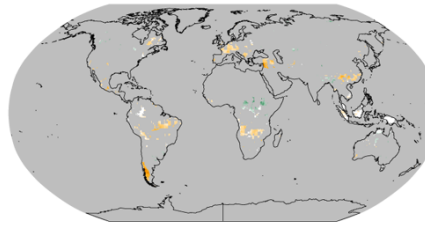
Interactive Discussion



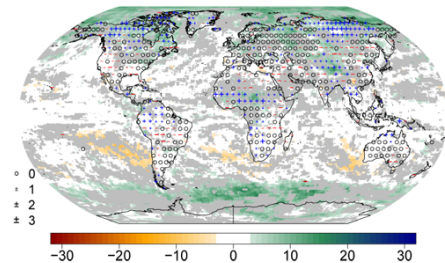
a SPI12 1950–2009 (CMIP5)



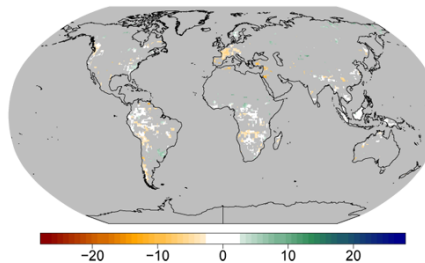
b SMA 1950–2009 (CMIP5)



c SPI12 1979–2009 (CMIP5)

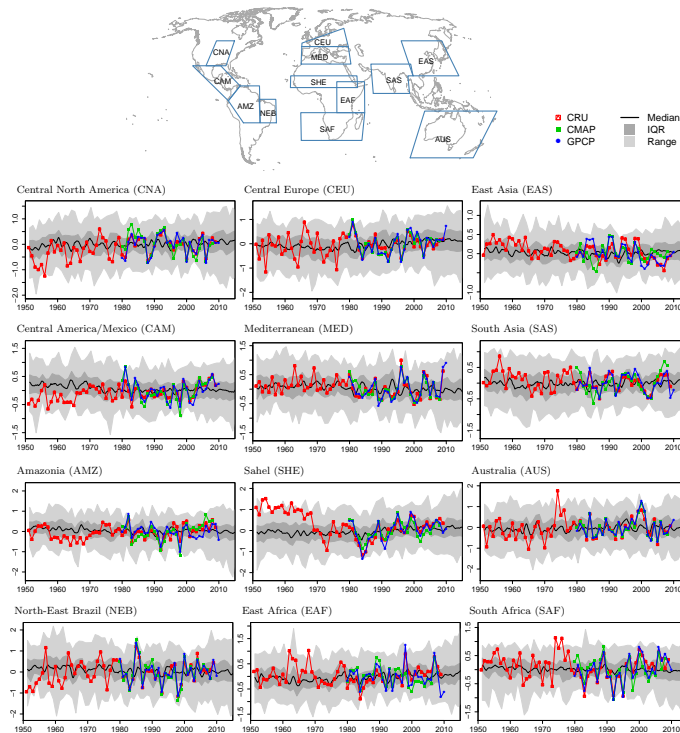


d SMA 1979–2009 (CMIP5)



**Fig. 2.** Consistency of drought trends in two observational periods (observations and CMIP5 GCM simulations) for SPI12 (**a, c**) and SMA (**b, d**). Colour shading is applied if the significant trends (evaluated at the 5% significance level) across the CMIP5 ensemble are all of the same sign and indicates the number of GCMs with significant trends (green-blue for positive, orange-red for negative trends). White indicates regions where at least 90% of the GCMs show no significant trends (consistently no change). All other areas are grey. Symbols in (**c**) show the same for three observational SPI12 datasets. “o”: none of the three datasets shows a significant trends; “+” and “-” indicate purely significant positive and negative trends, respectively; the size of the symbol indicates the number of agreeing observational datasets (see legend at **c**).

## Elusive drought

B. Orłowsky and  
S. I. Seneviratne

**Fig. 3.** Observed and CMIP5 simulated SPI12. Top: Spatial extent of the 12 regions considered in this study. Time series panels below: Annual averages of SPI12 values from three observational datasets (coloured lines) and median, inter-quartile range and total range across the CMIP5 ensemble (black line, dark grey and grey shading, respectively). Until 2005, CMIP5 data come from the *historical* simulations, after-wards, projections for the three GHG concentrations scenarios RCP2.6, RCP4.5 and RCP8.5 are combined. SPI12 values are calculated w.r.t. the 1979–2009 period for all datasets.

Title Page

Abstract

Introduction

Conclusions

References

Tables

Figures

◀

▶

◀

▶

Back

Close

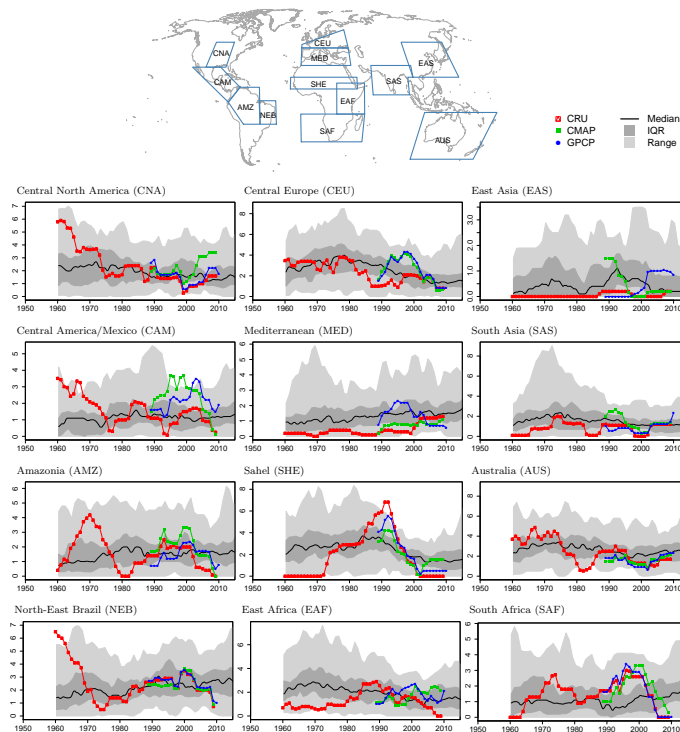
Full Screen / Esc

Printer-friendly Version

Interactive Discussion



## Elusive drought

B. Orłowsky and  
S. I. Seneviratne

**Fig. 4.** Occurrence frequencies of “mild drought” (SPI12 below  $-0.5$ ) in observations and CMIP5 simulations. Top: Spatial extent of the 12 regions considered in this study. Time series panels below: Occurrence frequencies of months per year with SPI12 below  $-0.5$ , calculated in 10-yr moving windows, from three observational datasets (coloured lines) and median, inter-quartile range and total range across the CMIP5 ensemble (black line, dark grey and grey shading, respectively). Until 2005, CMIP5 data come from the *historical* simulations, afterwards, projections for the three GHG concentrations scenarios RCP2.6, RCP4.5 and RCP8.5 are combined. SPI12 values are calculated w.r.t. the 1979–2009 period for all datasets.

Title Page

Abstract

Introduction

Conclusions

References

Tables

Figures

◀

▶

◀

▶

Back

Close

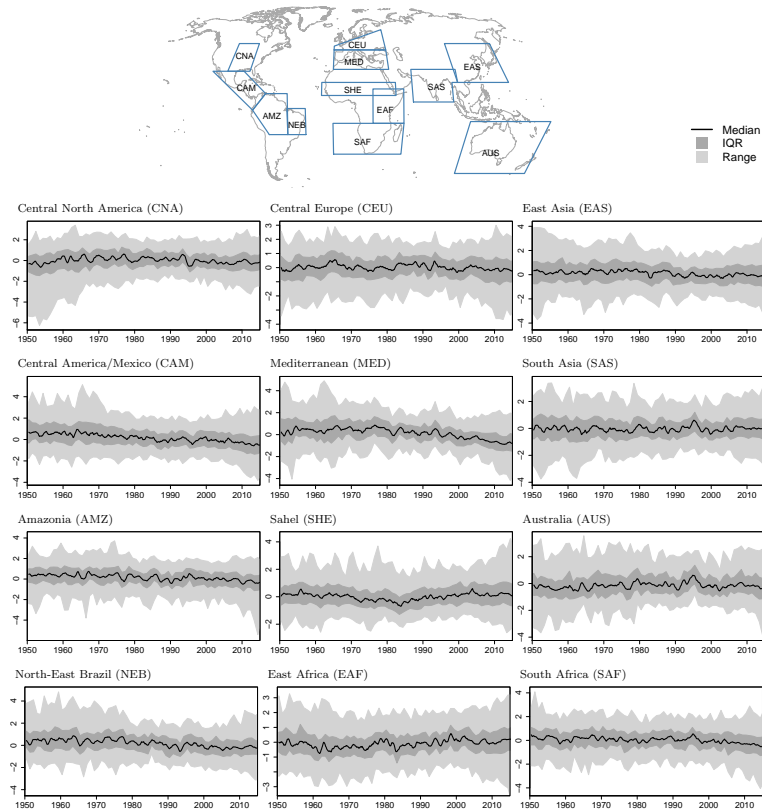
Full Screen / Esc

Printer-friendly Version

Interactive Discussion



## Elusive drought

B. Orłowsky and  
S. I. Seneviratne

**Fig. 5.** CMIP5 simulated SMA. Top: Spatial extent of the 12 regions considered in this study. Time series panels below: Median, inter-quartile range and total range across the CMIP5 ensemble of annual SMA averages (black line, dark grey and grey shading, respectively). Until 2005, CMIP5 data come from the *historical* simulations, after-wards, projections for the three GHG concentrations scenarios RCP2.6, RCP4.5 and RCP8.5 are combined. SMA values are calculated w.r.t. the 1979–2009 period for all datasets.

Title Page

Abstract

Introduction

Conclusions

References

Tables

Figures

◀

▶

◀

▶

Back

Close

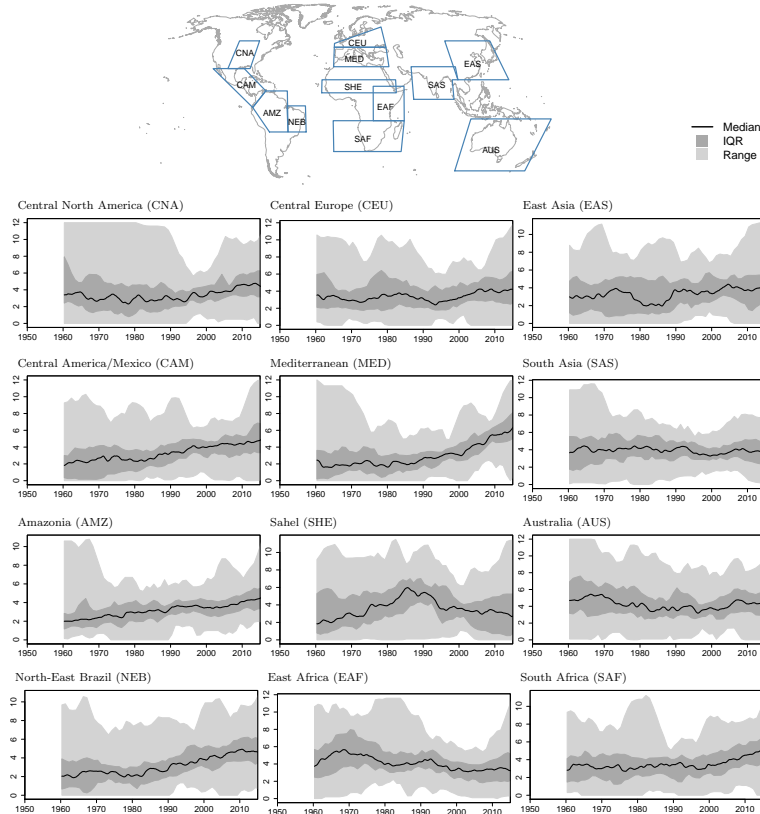
Full Screen / Esc

Printer-friendly Version

Interactive Discussion



## Elusive drought

B. Orlowsky and  
S. I. Seneviratne

**Fig. 6.** Occurrence frequencies of months with SMA below  $-0.5$  in CMIP5 simulations. Top: Spatial extent of the 12 regions considered in this study. Time series panels below: Median, inter-quartile range and total range across the CMIP5 ensemble (black line, dark grey and grey shading, respectively). Until 2005, CMIP5 data come from the *historical* simulations, afterwards, projections for the three GHG concentrations scenarios RCP2.6, RCP4.5 and RCP8.5 are combined. SMA values are calculated w.r.t. the 1979–2009 period for all datasets.

Title Page

Abstract

Introduction

Conclusions

References

Tables

Figures

◀

▶

◀

▶

Back

Close

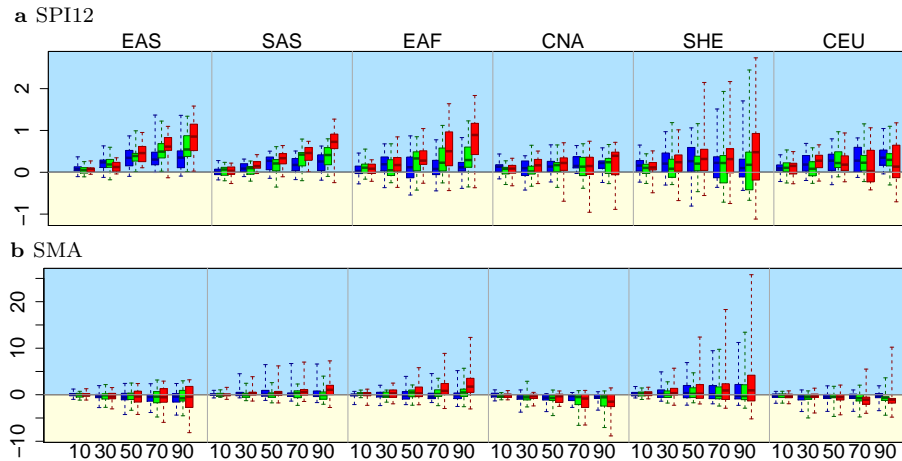
Full Screen / Esc

Printer-friendly Version

Interactive Discussion



## Elusive drought

B. Orłowsky and  
S. I. Seneviratne

**Fig. 7.** Wetting regions. **(a)** Box plots for 20-yr average 12-month Standardised Precipitation Indices (SPI12) in regions where SPI12 increases. The numbers at the bottom-most x-axis denote the central years in the 21st century of the 20-yr windows. Colours indicate the respective GHG concentrations scenario, blue: RCP2.6, green: RCP4.5 and red: RCP8.5. **(b)** like **(a)** but for Soil Moisture Anomalies (SMA). Changes are given as standard deviations w.r.t. 1979–2009 in both plots.

Title Page

Abstract

Introduction

Conclusions

References

Tables

Figures

◀

▶

◀

▶

Back

Close

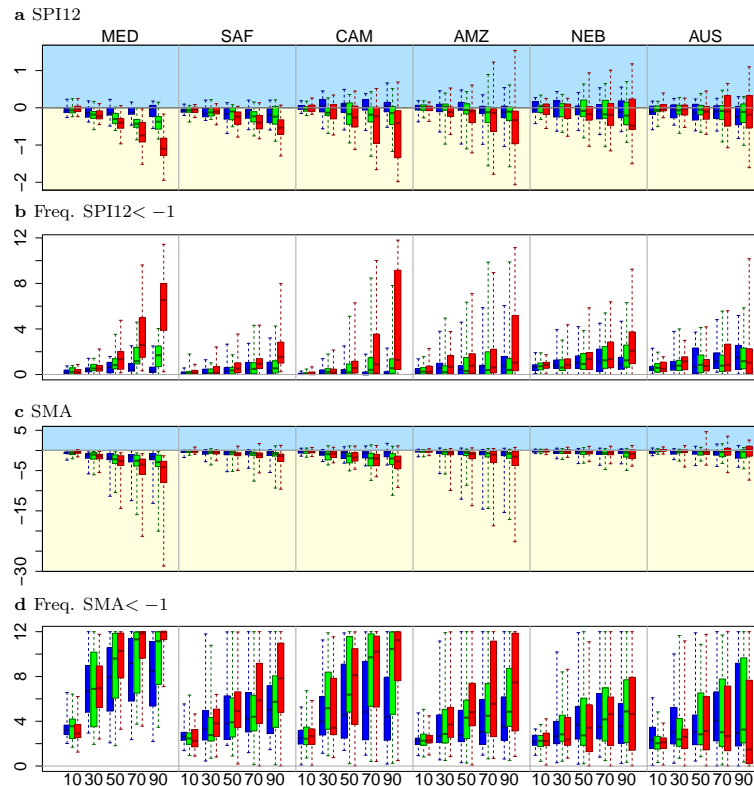
Full Screen / Esc

Printer-friendly Version

Interactive Discussion

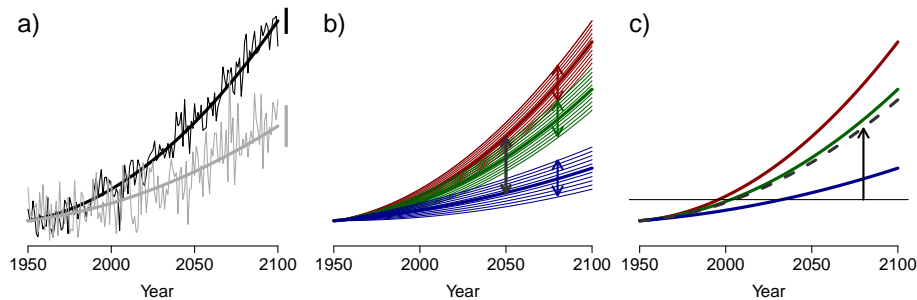


## Elusive drought

B. Orlowsky and  
S. I. Seneviratne

**Fig. 8.** Drying regions. **(a)** Box plots for 20-yr average 12-month Standardised Precipitation Indices (SPI12) in regions where SPI12 decreases. The numbers at the bottom-most x-axis denote the central years in the 21st century of the 20-yr windows. Colours indicate the respective GHG concentrations scenario, blue: RCP2.6, green: RCP4.5 and red: RCP8.5. **(b)** Months per year in which SPI12 drops below  $-1$ , calculated for moving 10-yr windows. **(c)** and **(d)** Like **(a)** and **(b)** but for Soil Moisture Anomalies (SMA). Changes are given as standard deviations w.r.t. 1979–2009 in **(a)** and **(c)** and as months per year in **(b)** and **(d)**.

## Elusive drought

B. Orlowsky and  
S. I. Seneviratne

**Fig. 9.** Separation of the overall ensemble uncertainty  $\sqrt{T_t}$  into relative contributions from internal variability  $V$ , uncertainty due to GCM formulation  $M_t$  and GHG concentrations scenario  $S_t$  following Hawkins and Sutton (2009). **(a)** Two illustrative GCM time series and their 4th order polynomial fit. The bars to the right denote the time-independent variability of the residuals. Their average over all GCM series and GHG concentrations scenarios defines the internal variability,  $V$ . **(b)** Illustrative 4th order polynomial fits of GCM time series from three different GHG concentrations scenarios (colours blue, green, red). Thick lines denote the averaged time series of the series corresponding to each of the different GHG concentrations scenarios. Coloured arrows indicate the variability within each scenario at a given year. Their average defines the uncertainty due to GCM formulation,  $M_t$ , for that year. The grey arrow indicates the variability of the intra-scenario average time series at a given year. This variability defines the uncertainty due to GHG concentrations scenario,  $S_t$ . **(c)** The intra-scenario averages and their mean (black dashed line). The change signal of a given year,  $G_t$ , is defined as the change in this mean w.r.t. the level of the reference year 2006 (horizontal line). See text for details.

Title Page

Abstract

Introduction

Conclusions

References

Tables

Figures

◀

▶

◀

▶

Back

Close

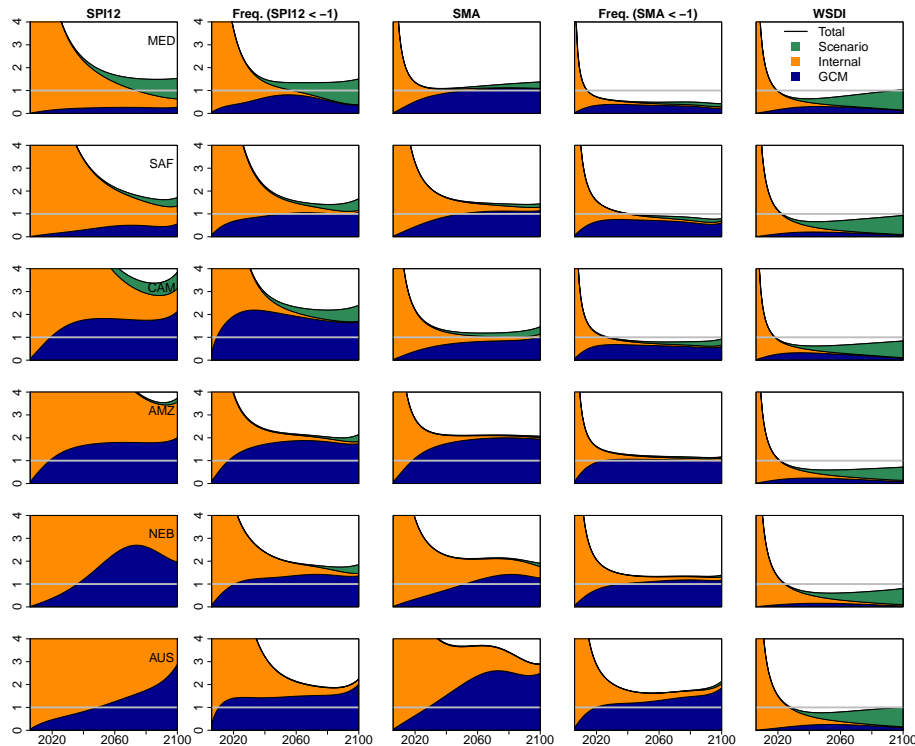
Full Screen / Esc

Printer-friendly Version

Interactive Discussion



## Elusive drought

B. Orłowsky and  
S. I. Seneviratne

**Fig. 10.** Fractional uncertainty, defined as uncertainty divided by the change since 2006,  $F_t = \sqrt{T_t}/G_t$ . Columns show  $F_t$  for magnitude and frequency (months per year with values below  $-1$ , calculated from 10-yr moving windows) of SPI12, SMA and a heat wave indicator (WSDI) for the analysed hot spot regions with increasing SPI12 (rows). Colours indicate the relative uncertainty contributions from GCM formulation ( $M_t$ , blue), internal variability ( $V$ , orange) and GHG concentrations scenarios ( $S_t$ , green). See Fig. 9 and text for details.